Uncovering the chemical enrichment and mass-assembly histories of star-forming galaxies

R. Cid Fernandes[1], N. V. Asari[1], L. Sodré Jr.[2], G. Stasińska [3], A. Mateus[2], J. P. Torres-Papaqui[1], W. Schoenell [1]

[1]*Departamento de Física - CFM - Universidade Federal de Santa Catarina, Florianópolis, SC, Brazil*
[2]*Instituto de Astronomia, Geofísica e Ciências Atmosféricas, Universidade de São Paulo, São Paulo, SP, Brazil*
[3]*LUTH, Observatoire de Meudon, 92195 Meudon Cedex, France*

5 February 2008

ABSTRACT

We explore the mass-assembly and chemical enrichment histories of star forming galaxies by applying a population synthesis method to a sample of 84828 galaxies from the Sloan Digital Sky Survey Data Release 5. Our method decomposes the entire observed spectrum in terms of a sum of simple stellar populations spanning a wide range of ages and metallicities, thus allowing the reconstruction of galaxy histories. A comparative study of galaxy evolution is presented, where galaxies are grouped onto bins of nebular abundances or mass. We find that galaxies whose warm interstellar medium is poor in heavy elements are slow in forming stars. Their stellar metallicities also rise slowly with time, reaching their current values ($Z_\star \sim 1/3 Z_\odot$) in the last ~ 100 Myr of evolution. Systems with metal rich nebulae, on the other hand, assembled most of their mass and completed their chemical evolution long ago, reaching $Z_\star \sim Z_\odot$ already at lookback times of several Gyr. These same trends, which are ultimately a consequence of galaxy downsizing, appear when galaxies are grouped according to their stellar mass. The reconstruction of galaxy histories to this level of detail out of integrated spectra offers promising prospects in the field of galaxy evolution theories.

Key words: galaxies: evolution - galaxies: stellar content - galaxies: statistics

1 INTRODUCTION

One of the major challenges of modern astrophysics is to understand the physical processes involved in galaxy formation and evolution. Significant steps in this direction could be made by tracing the build up of stellar mass and metallicity as a function of cosmic time.

One way to address this issue is through cosmologically deep surveys which map how galaxy properties change for samples at different redshifts (z). Among these properties, the relation first observed by Lequeux et al. (1979) between heavy-element nebular abundance and galaxy mass, or its extension, the luminosity-metallicity relation (e.g., Skillman et al. 1989; Zaritsky et al. 1994), are being extensively used to probe the metal enrichment along cosmic history. Clear signs of evolution are being revealed by studies of these relations at both intermediate (Savaglio et al. 2005; Lamareille et al. 2006; Mouhcine et al. 2006) and high z (Shapley et al. 2005; Maier et al. 2006; Erb et al. 2006), which generally find significant offsets in these relations when compared to their versions in the local Universe.

Alternatively, one may study galaxy evolution through *fossil* methods, which reconstruct the star formation history (SFH) of a galaxy from the properties of their stars. The most detailed studies of this sort are those based on nearby galaxies (including our own), where color-magnitude diagrams and even spectroscopy of individual stars are feasible (e.g., Smecker-Hane et al. 1996; Hernandez et al. 2000; Dolphin 2002; Rizzi et al. 2003; Skillman et al. 2003; Monaco et al. 2005; Koch et al. 2005). Comparing such observations with predictions of evolutionary synthesis models then allows one to infer how stars were born as a function of time, as well as to constrain the chemical enrichment histories of the galaxies (e.g., Lanfranchi, Matteucci & Cescutti 2006; Carigi, Colín & Peimbert 2006). By mapping how stars become richer in metals as a galaxy ages, these studies provide useful constraints for chemical evolution models.

Beyond the local group and its neighborhood, fossil methods must derive SFHs from integrated galaxy spectra, using either selected spectral features (Kauffmann et al. 2004; Brinchmann et al. 2004; Gallazzi et al. 2005; Nelan et al. 2005; Thomas et al. 2005; Bernardi et al. 2006) or the full spectrum (Panter, Heavens & Jimenez 2003; Heavens et al. 2004; Cid Fernandes et al. 2005; Mathis, Charlot & Brinchmann 2006; Panter et al. 2006). This approach works

with much less information than is available from individual stars in galaxies, so one cannot expect similar levels of accuracy. On the other hand, integrated spectra of galaxies are now available by the hundreds of thousands from modern spectroscopic surveys, so the decrease in accuracy is compensated by orders of magnitude increase in statistics and by the broader range in galaxy types spanned by such surveys. It is therefore of great interest to explore methods to retrieve information on galaxy evolution from integrated spectroscopic data.

In our ongoing series of papers entitled the Semi Empirical Analysis of Sloan Digital Sky Survey (SDSS) Galaxies, (Cid Fernandes et al. 2005; Mateus et al. 2006a; Stasińska et al. 2006; Mateus et al. 2006b; SEAGal I–IV, respectively) we have shown that a decomposition of galaxy spectra in terms of instantaneous bursts of different ages ($t_\star$) and metallicities ($Z_\star$) produces both excellent spectral fits and astrophysically meaningful results. So far, however, our description of SFHs has been extremely sketchy, based on averages over the $t_\star$ and $Z_\star$ distributions, thus washing out valuable time-dependent information.

This paper shows that we can actually do much better. To illustrate this we have culled a sample of star-forming (SF) galaxies from the SDSS (Section 2), to which we apply our synthesis method and derive mass-assembly and chemical enrichment histories (Section 3). The evolution of stellar mass and metallicity is then studied by grouping galaxies with similar nebular abundances or mass (Section 4). Details of this analysis and cross-checks on the results reported here are presented in a companion paper (Asari et al. , in prep, hereafter A07).

2   DATA

We have recently completed detailed pixel-by-pixel spectral fits of 573141 galaxies from the Main Galaxy Sample of the SDSS Data Release 5 (Adelman-McCarthy et al. 2006) with the synthesis code STARLIGHT described in SEAGal I and II. STARLIGHT decomposes an observed spectrum in terms of a sum of simple stellar populations covering a grid of 25 ages from $t_{\star,j} = 1$ Myr to 18 Gyr and 6 metallicities $Z_{\star,j} = 0.0001$ to 0.05 (ie, from 0.005 to 2.5 $Z_\odot$). Each of these $N_\star = 150$ instantaneous bursts is represented by a spectrum extracted from the evolutionary synthesis models of Bruzual & Charlot (2003) for a Chabrier (2003) initial mass function, Padova 1994 tracks, and STELIB library (Le Borgne et al. 2003). Illustrative fits are presented in SEAGal I and A07.

Emission lines were measured from the starlight subtracted spectra. Figure 1a shows the Baldwin, Phillips & Terlevich (1981, BPT) diagnostic diagram for 175234 galaxies for which Hβ, [OIII]λ5007, Hα and [NII]λ6584 are all detected with $S/N \geq 3$. Reddening corrected line fluxes are used in this plot and throughout our analysis. The distribution of points in this diagram resembles a flying seagull, with SF galaxies occupying the left wing and galaxies hosting an AGN on the right. We define SF galaxies as those under the divisory line proposed in SEAGal III (solid line in Figure 1a). Further requiring a minimum continuum S/N of 10 at ~ 4750 Å leaves a set of 84828 objects, hereafter the SF-sample, shown in Figure 1b. Results for alternative

sample definitions (involving different S/N thresholds, other AGN/SF separation criteria, and cuts on galaxy inclination) are presented in A07. Note that by selecting SF galaxies we indirectly select spirals over elliptical galaxies.

The SF-wing is essentially a sequence in nebular metallicity (SEAGal III and references therein), which we quantify by the oxygen abundance obtained through the strong-line calibration of Stasińska (2006):

$$\log Z_{neb} = \log \frac{(O/H)}{(O/H)_\odot} = -0.14 - 0.25 \log \frac{[OIII]\lambda5007}{[NII]\lambda6584} \quad (1)$$

where $(O/H)_\odot = 4.9 \times 10^{-4}$ (Allende Prieto, Lambert & Asplund 2001). We believe this is the most reliable calibration available in the literature, since it is based on temperature-based abundances in the metal-poor case and on the ([OII] + [OIII])/Hβ calibration of Pilyugin (2000) in the metal-rich regime, using a large sample of giant HII regions.

Z_{neb} is both a physically motivated and mathematically convenient coordinate to map galaxy positions along the left wing in the BPT diagram. From the tip of the SF-wing in Fig 1a to its bottom, our SF sample spans the $Z_{neb} \sim 0.2$–1.6 $Z_\odot$ range. In Fig 1b this interval is chopped onto 6 logarithmic bins of width $\Delta \log Z_{neb} = 0.13$ dex, except for the first one which is twice as wide to include more sources. Galaxies inside these same bins will be grouped together in the analysis of star-formation and chemical enrichment histories presented in the following.

3   METHOD OF ANALYSIS

As thoroughly discussed in the literature on stellar population synthesis, the combination of noise in the data, astrophysical and mathematical degeneracies limits the amount of information about galactic histories that can be extracted from integrated spectra. Clearly, the 150 components of the population vector used in our fits are a greatly over-detailed description, so some *a posteriori* compression of the results to a lower dimension is needed. Our previous papers (SEAGal I–IV) have taken this compression approach to its extreme by reducing the whole $t_\star$ and $Z_\star$ distributions encoded in the population vector to their first moments,

$$\langle \log t_\star \rangle_M = \sum_{j=1}^{N_\star} \mu_j \log t_{\star,j} \quad (2)$$

$$\langle Z_\star \rangle_M = \sum_{j=1}^{N_\star} \mu_j Z_{\star,j} \quad (3)$$

where μ_j is the fraction of the total stellar mass ($M_\star$) which is in the jth population.

Both $\langle \log t_\star \rangle$ and $\langle Z_\star \rangle$ proved to be mathematically robust and astrophysically valuable summaries of the full population vector. In SEAGal I, II and A07 these averages are shown to cleanly reveal important relations, such as those between $\langle \log t_\star \rangle$ and $M_\star$ (associated with the galaxy downsizing phenomenon), $\langle Z_\star \rangle$ and $M_\star$ (the mass-metallicity relation), and $\langle Z_\star \rangle$ and Z_{neb} (which reveals a connection between stellar and nebular chemical enrichment levels). Given this success, it is natural to explore less drastic compressions of the population vector.
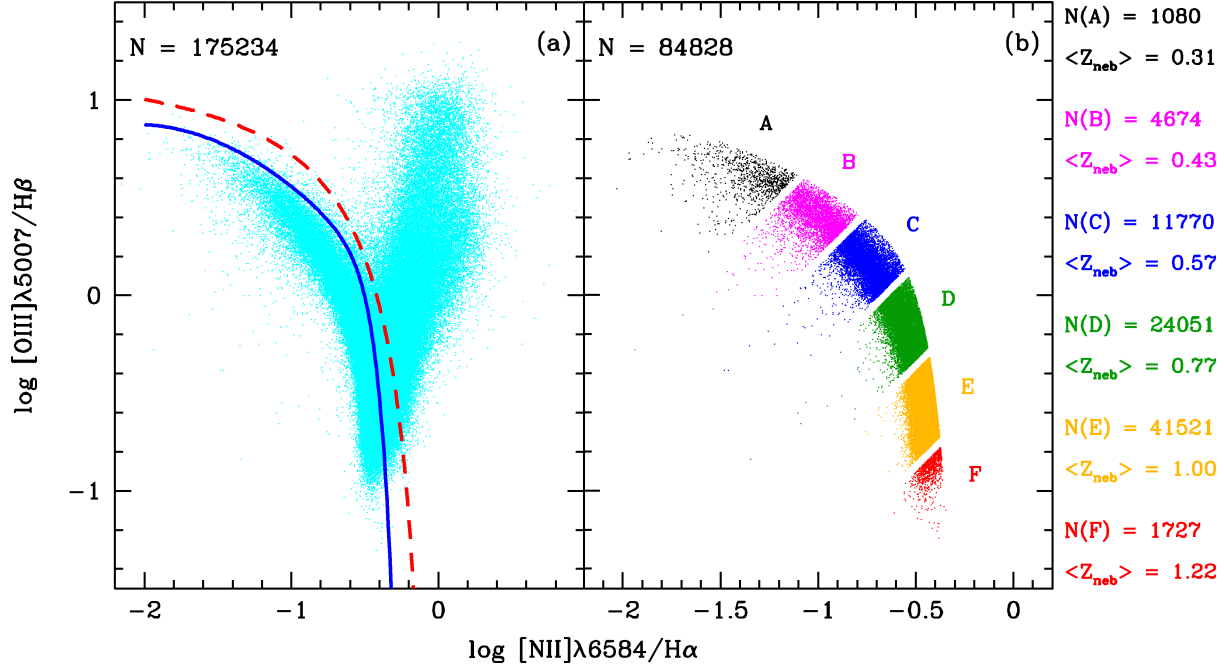
Figure 1. (a) 175234 SDSS galaxies in the BPT diagram. The solid line (Stasińska et al 2006) divides Star-Forming galaxies from those hosting AGN. The dashed line shows the dividing line used by Kauffmann et al. (2003). (b) The SF sample, chopped into six bins of nebular abundance. The number of galaxies in each bin is given in the right, along with the corresponding mean Z_{neb} values (in solar units). Galaxies close to bin borders are not plotted for clarity.

One way to compress the population vector but retain the age-information is to marginalize over the $Z_{\star,j}$ distribution and compute the total mass converted into stars as a function of time:

$$\eta_\star^c(t_\star) = \sum_{t_{\star,j} > t_\star} \mu_j^c \qquad (4)$$

where μ_j^c denotes the fraction of the total mass converted onto stars $(M_\star^c)$ that is associated with the jth base age. The superscript "c" stands for "converted onto stars", and is introduced to distinguish μ_j^c and $M_\star^c$ from μ_j and $M_\star$, which refer to the mass still locked inside stars, ie, discounting the mass returned to the inter-stellar medium (ISM) by stellar evolution. $\eta_\star^c(t_\star)$ is thus a monotonic function which grows from 0 to 1 as $t_\star$ runs from the time galaxy formation starts to the present, and maps what fraction of $M_\star^c$ was assembled up to a given lookback time.[1]

To track the evolution of the *stellar metallicity* we compute the total mass in metals inside stars as a function of $t_\star$ and divide it by the total mass inside stars at the same time. This yields the time-dependent mean stellar metallicity:

$$\overline{Z_\star}(t_\star) = \sum_{t_{\star,j} > t_\star} \mu_j(t_\star) Z_{\star,j} \qquad (5)$$

The computation of $\mu_j(t_\star)$ takes into account that the total mass inside stars changes with time, both due to the SFH

and to the time dependence of the returned mass. Accordingly, only populations older than $t_\star$ enter the definition of $\mu_j(t_\star)$, since younger ones had not formed yet, ie., $\mu_j(t_\star) = 0$ for $t_{\star,j} < t_\star$.

4 RESULTS

The explicit time-dependence in equations (4) and (5) provides a description of the star formation and chemical histories of galaxies which goes well beyond that obtained with the mere first moments of the age and metallicity distributions. Given the numerous degeneracies which affect population synthesis of galaxy spectra one might be skeptical as to how useful they actually are. Simulations addressing this issue will be presented elsewhere. In what follows we report what is obtained in practice.

4.1 Galaxy evolution in Z_{neb}-bins

Our strategy is to chop the SF-wing into bins in Z_{neb} and study the evolution of galaxies from the statistics of $\eta_\star^c(t_\star)$ and $\overline{Z_\star}(t_\star)$ in each bin. The fact that Z_{neb} correlates strongly with several physical and observational properties guarantees that galaxies inside each Z_{neb} bin are intrinsically similar, which in turn implies that statistics over such bins is meaningful.

Fig 2a shows the mean mass-assembly functions obtained for each of the six Z_{neb} bins illustrated in Fig 1b. The systematics is evident to the eye. Galaxies with low Z_{neb} are slower in assembling their stars than those with high Z_{neb}. This behavior reflects the fact that, although most of the mass is assembled at early times ($t_\star \gtrsim 1$ Gyr), galaxies

---

[1] Since our main goal is to compare the *intrinsic* evolution of galaxies, throughout this letter we consider ages in the context of stellar-evolution alone, ie., as if all galaxies were observed at $z = 0$, such that $t_\star$ is both a stellar-age and a lookback time.
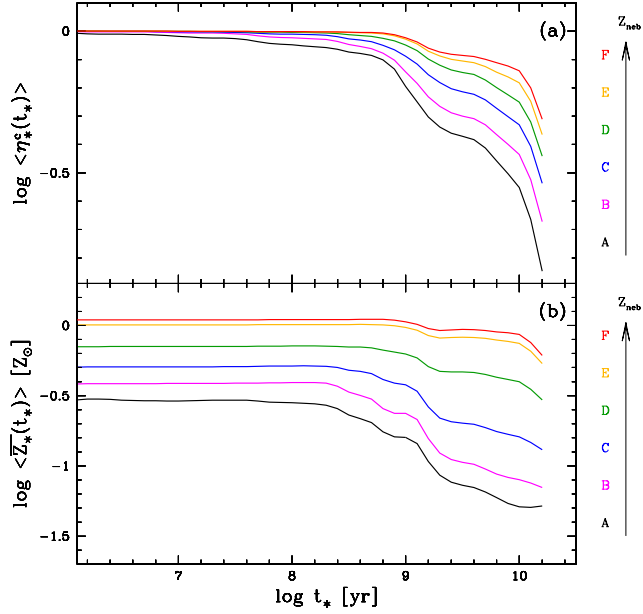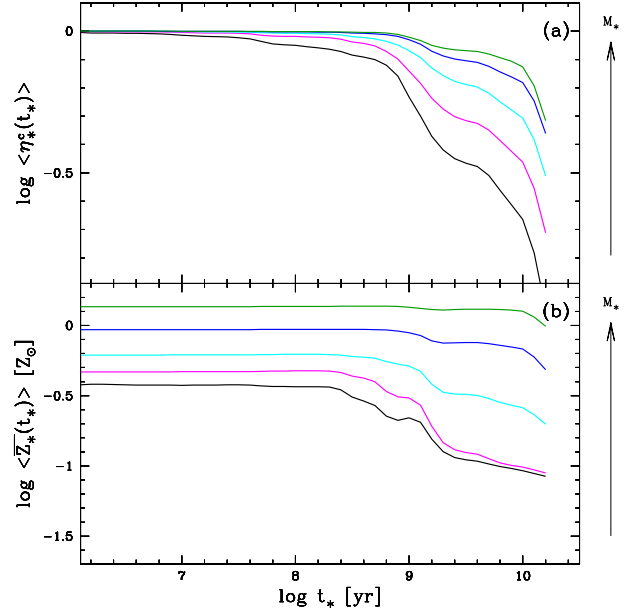
Figure 2. (a) Average mass assembly ($\eta_\star^c$) and (b) chemical evolution ($\overline{Z_\star}$) of stars in SF galaxies for the same six Z_{neb}-bins defined in Fig 1b. Each line represents a $t_\star$-by-$t_\star$ average over all galaxies in the bin. A mild gaussian smoothing with FWHM = 0.2 dex in $\log t_\star$ was applied to the mean $\eta_\star^c(t_\star)$ and $\overline{Z_\star}(t_\star)$ curves, just enough to smooth out discreteness effects associated to the 25 ages in the base.

Figure 3. As Fig 2, but binning SF galaxies by their stellar mass, using five 1 dex wide bins, centered at (from bottom to top) $\log M_\star/M_\odot = 7.5$, 8.5, 9.5, 10.5 and 11.5, which contain 583, 4750, 29056, 46847 and 3550 galaxies, respectively.

at the tip of the SF-wing have larger star formation rates (SFR) per unit mass in the recent past than those at the bottom of the wing. This trend can be quantified in terms the ratio of the mean SFR in the last 60 Myr to that over the galaxy's history, ie, the so called Scalo's b parameter (eg, Brinchmann et al. 2004). We find b to decrease by a factor of ~ 20 from the lower to the higher Z_{neb} bins. (SFRs are discussed in A07, where it is also shown that our synthesis based SFRs agree very well with those derived from the Hα luminosity.) Alternatively, one may quantify this behavior by computing the time at which the mean $\eta_\star^c(t_\star)$ function reaches 0.75, ie., the time at which the mass involved in star-formation reaches 3/4 of the total. We find that τ_{75} increases from ~ 0.8 Gyr at $Z_{neb} \sim 0.31$ (bin A in Fig 1b), to 2 Gyr at $Z_{neb} \sim 0.77 Z_\odot$ (bin D), and 8 Gyr for the highest Z_{neb} bin. Given that Z_{neb} correlates strongly with $M_\star$ (Zaritsky et al. 2004; Tremonti et al. 2004; Lee et al. 2006), this behavior is ultimately a signature of galaxy downsizing (Cowie et al. 1996).

The chemical evolution of stars in SF galaxies is shown in Fig 2b. Again, the main message is clear: Galaxies with a metal poor ISM are low are slow in their stellar chemical enrichment. In the lower Z_{neb} bins, $\overline{Z_\star}(t_\star)$ only reaches the current stellar metallicity level ($\sim 1/3 Z_\odot$) as recently as $t_\star \sim 100$ Myr. Galaxies with larger Z_{neb}, on the other hand, have flatter and systematically higher $\overline{Z_\star}(t_\star)$ curves. These massive systems have essentially completed their mass assembly and chemical evolution long ago, so that recent star-forming activity has a negligible impact upon $\overline{Z_\star}(t_\star)$.

The fact that bins of increasing Z_{neb} have increasingly

higher present $\overline{Z_\star}$ values confirms that nebular and stellar metallicities are related (SEAGal I; Gallazzi et al. 2005; A07). We nevertheless warn the reader not to overinterpret the quantitative relation between these two quantities, given that they are derived by completely different and hardly comparable means. In this paper we use [OIII]/[NII] as an indicator of Z_{neb} (equation 1), because of its evident relation to the position of the points in the BPT diagram. However, as emphasized by Stasińska (2006), strong line methods for deriving nebular abundances have been calibrated using giant HII regions and their relevance for integrated spectra of galaxies has still to be examined, because of the role of metallicity gradients and of the diffuse ionized medium in galaxies. In addition, there is so far no study comparing nebular abundance calibrations with stellar abundances. Therefore, our Z_{neb} values are not necessarily on the same scale as stellar abundances. Insofar as this paper is concerned, this is not a problem, since, irrespective of absolute values, it is the existence of a Z_{neb}-$\overline{Z_\star}$ relation which is responsible for the ordering of the different chemical evolution curves in Fig 2b.

4.2 Galaxy evolution in Mass-bins

While Fig 2 illustrates the strong link between the stellar mass assembly and chemical evolution histories of galaxies and the present ionized ISM metal content, Z_{neb} is not the cause, but the product of galaxy evolution, so its use as an independent variable, although pedagogically useful, is questionable. If one had to chose a single quantity as the main driver of galaxy evolution this would surely be its mass (eg., Tinsley 1968; Larson 1974; Pagel 1997).

We have thus repeated the analysis above binning galax-

ies by $M_\star$ instead of Z_{neb}. Results are shown in Fig 3 for five 1 dex-wide mass bins centered at $\log M_\star/M_\odot = 7.5 \ldots 11.5$. Because of the flattening of the $M_\star - Z_{neb}$ relation at high masses and the substantial scatter around the relation, particularly at low $M_\star$ and Z_{neb}, binning in $M_\star$ or Z_{neb} samples somewhat different populations of galaxies. On the whole, however, this alternative grouping scheme leads to the same general scenario outlined above, with low $M_\star$ galaxies being slower in their mass and chemical build up than more massive ones. A caveat is that $M_\star$ is not a perfect tracer of the depth of the potential well, since it does not account for the mass in gas nor dark matter. In any case, the signature of galaxy downsizing is evident in Fig 3: massive galaxies today formed most of their stars and metals long time ago, whereas low-mass galaxies are still forming stars and metals actively.

The signal of chemical evolution is present in all curves in Figs 2b and 3b. Curiously, however, this evolution does not seem to start from very low $\overline{Z_\star}$ for massive, high Z_{neb} galaxies (eg, bins E and F). We interpret this apparent lack of old, metal poor populations as due to a combination of lack of age resolution at high $t_\star$ and an intrinsically fast evolution ocurring at early times. In low mass systems (eg, bin A), $\overline{Z_\star}(t_\star)$ starts is $\Delta t_\star \sim 2$ Gyr long rise period at $t_\star \sim 2$–3 Gyr, such that $\Delta t_\star/t_\star$ is of order unity. The same process happening at $t_\star > 10$ Gyr would yield $\Delta t_\star/t_\star < 0.2$, and consequently be much harder to resolve. As shown above above, by $t_\star = 10$ Gyr massive galaxies had already assembled most of their mass, so their chemical evolution must also have occurred early on. This mixture of populations of widely different metallicities but similar ages results in $\overline{Z_\star}$ values at $t_\star > 10$ Gyr which are dominated by the metal rich stars already present at those times. Such an early and rapid formation period should lead to enhancement of elements synthesized in type II SNe (Worthey, Faber & González 1992; Thomas et al. 2005). Though we cannot map elemental abundances with our method, we do detect a signal of increasing α enhancement towards the bottom of the BPT diagram by means of systematically increasing residuals in spectral bands due to α elements like Mg (A07), indirectly supporting the scenario outlined above.

5 CONCLUDING REMARKS

Our analysis shows that the present ISM abundance is intimately connected to the past star-formation and chemical enrichment history of a galaxy. Whereas this is intuitively obvious from a physical point of view, it is not obvious at all that one should be able to recover this behavior from population synthesis analysis of integrated galaxy spectra of SDSS-like quality. We emphasize that, unlike previous studies such as that by Bica (1988), our fits impose no *a priori* chemical evolution constraints whatsoever upon the mixture of $t_{\star,j}$'s and $Z_{\star,j}$'s in the base. Given the absence of constraints and the fact that the fits are completely independent of the emission line data used to compute Z_{neb}, the organization of galaxies with different Z_{neb} onto the clear and systematically distinct stellar chemical enrichment patterns seen in Fig 2b is remarkable, revealing that fossil methods based on integrated spectra have reached a level of maturity which would be unthinkable just a few years ago (eg,

Cid Fernandes et al. 2001). By taking the spectral synthesis output one step further than the trivial first moments of the $t_\star$ and $Z_\star$ distributions, we have been able to uncover the chemical evolution of galaxies with an unprecedented level of detail for such a large and varied sample. This significant achievement was only possible due to the fabulous statistics of the SDSS, combined with state-of-the-art evolutionary synthesis models and reliable SFH recovery techniques. The sheer number of galaxies allows us to recover an unequivocal chemical evolution signal which would be at best doubtful for individual galaxies or even small samples. Combined with our estimates of the star-formation histories, the empirically derived chemical evolution patterns should provide valuable constraints for galaxy evolution models.

REFERENCES

Adelman-McCarthy J.K., et al. , 2006, in preparation
Allende Prieto C., Lambert D. L., Asplund M., 2001, ApJ, 556, L63
Asari N. V., et al. , 2007, in preparation
Baldwin J. A., Phillips M. M., Terlevich R., 1981, PASP, 93, 5
Bernardi M., Nichol R. C., Sheth R. K., Miller C. J., Brinkmann J., 2006, AJ, 131, 1288
Bica E., 1988, A&A, 195, 76
Brinchmann J., Charlot S., White S. D. M., Tremonti C., Kauffmann G., Heckman T., Brinkmann J., 2004, MNRAS, 351, 1151
Bruzual G., Charlot S., 2003, MNRAS, 344, 1000
Carigi L., Colín P., Peimbert M., 2006, ApJ, 644, 924
Chabrier G., 2003, PASP, 115, 763
Cid Fernandes R., Sodré L., Schmitt H. R., Leão J. R. S., 2001, MNRAS, 325, 60
Cid Fernandes R., Mateus A., Sodré L., Stasińska G., Gomes J. M., 2005, MNRAS, 348, 363 (SEAGal I)
Cowie L.L., Songaila A., Hu E.M., Cohen J.G., 1996, AJ, 112, 839
Dolphin A. E., 2002, MNRAS, 332, 91
Erb D. K., Shapley A. E., Pettini M., Steidel C. C., Reddy N. A., Adelberger K. L., 2006 ApJ, 644, 813
Gallazzi A., Charlot S., Brinchmann J., White S. D. M., Tremonti C. A., 2005, MNRAS, 362, 41

Heavens A. F., Panter B., Jimenez R., Dunlop J., 2004, Nature, 428, 625

Hernandez X., Gilmore G., Valls-Gabaud D., 2000, MNRAS, 317, 831

Kauffmann G., et al. , 2003, MNRAS, 346, 1055

Kauffmann G., White S. D. M., Heckman T. M., Ménard B., Brinchmann J., Charlot S., Tremonti C., Brinkmann J., 2004, MNRAS, 353, 713

Koch A., Grebel E. K., Wyse R. F. G, Kleyna J. T., Wilkinson M. I., Harbeck D., Gilmore G. F., Evans N. W., 2006, accepted in the AJ, (astro-ph/0511087)

Lamareille F., Contini T., Brinchmann J., Le Borgne J. F., Charlot S., Richard J., 2006, A&A, 448, 907

Lanfranchi G. A., Matteucci F., Cescutti G., 2006, A&A, 453, 67

Larson R. B., 1974, MNRAS, 166, 585

Le Borgne J. F., et al. , 2003, A&A, 402, 433

Lee H., Skillman E. D., Cannon J. M., Jackson D. C., Gehrz R. D., Polomski E. F., Woodward C. E., 2006, ApJ, 647, 970

Lequeux J., Peimbert M., Rayo J. F., Serrano A., Torres-Peimbert S., 1979, A&A, 80, 155

Maier C., Lilly S. J., Carollo C. M., Meisenheimer K., Hippelein, H., Stockton A., 2006, ApJ, 639, 858

Mateus A., Sodré L., Cid Fernandes R., Stasińska G., Schoenell W., Gomes J. M., 2006a, MNRAS, 370, 721 (SEAGal II)

Mateus A., Sodré L., Cid Fernandes R., Stasińska G., 2006b, submitted to MNRAS, (astro-ph/0604063) (SEAGal (IV))

Mathis H., Charlot S., Brinchmann J., 2006, MNRAS, 365, 385

Monaco L., Bellazzini M., Bonifacio P., Ferraro F. R., Marconi G., Pancino E., Sbordone L., Zaggia S., 2005, A&A, 441, 141

Mouhcine M., Bamford S. P., Aragón-Salamanca A., Nakamura O., Milvang-Jensen B., 2006, MNRAS, 369, 891

Nelan J. E., Smith R. J., Hudson M. J., Wegner G. A., Lucey J. R., Moore S. A. W., Quinney S. J., Suntzeff N. B., 2005, ApJ, 632, 137

Pagel B. E. J., 1997, Nucleosynthesis and chemical evolution of galaxies, Cambridge University Press

Panter B., Heavens A. F., Jimenez R., 2003, MNRAS, 343, 1145

Panter B., Jimenez R., Heavens A.F., Charlot S., 2006, Submitted to MNRAS, (astro-ph/0608531)

Pilyugin, L. S. 2000, A&A, 362, 325

Rizzi L., Held E. V., Bertelli G., Saviane I., 2003, ApJ, 589, L85

Savaglio S., et al. , 2005, ApJ, 635, 260

Shapley A. E., Coil A. L., Ma Chung-Pei, Bundy K., 2005, ApJ, 635, 1006

Skillman E. D., Kennicutt R. C., Hodge P. W., 1989, ApJ, 347, 875

Skillman E. D., Tolstoy E., Cole A. A., Dolphin A. E., Saha A., Gallagher J. S., Dohm-Palmer R. C., Mateo M., 2003, ApJ, 596, 253

Smecker-Hane T. A., Gallagher J. S., Hodge P., Stetson P. B., 1996, AAS, 188, 6502

Stasińkska G., Cid Fernandes R., Mateus A., Sodré L., Asari N. V., 2006, MNRAS, 371, 972 (SEAGal III)

Thomas D., Maraston C., Bender R., Mendes de Oliveira C.,2005, ApJ, 621, 673

Tinsley B. M., ApJ, 151, 547

Tremonti, C. A., et al. ., 2004, ApJ, 613, 898

Worthey G., Faber S. M., Gonzalez J. J., 1992, ApJ, 398, 69

Zaritsky D., Kennicutt R. C., Huchra J. P., 1994, ApJ, 420, 87

Zaritsky D., Gonzalez A. H., Zabludoff A. I., 2004, ApJ, 613, L93